Anchor Pile Design for Floating Offshore Wind Turbines

Charlie Aaron Spicer, C N Abadie, Gopal Madabhushi

ICONHIC2022
3rd International Conference on Natural Hazards & Infrastructure
5-7 July 2022, Athens, Greece

Anchor Pile Design for Floating Offshore Wind Turbines

Charles Aaron Spicer, Dr Christelle Nadine Abadie, Professor Gopal Santana Phani Madabhushi
Department of Engineering, University of Cambridge

ABSTRACT

As the world is working towards accelerating the global transition to clean power, the development of floating offshore wind turbine (FOWT) technologies is becoming increasingly important. The design of robust anchors that can sustain severe cyclic loads from the wind, waves and currents, for a large number of cycles, is central to the deployment of future floating wind farms. This paper presents experimental work to further understand and improve the design of driven anchor piles in sandy soils for Tension Leg Platforms (TLPs). It involves laboratory tests at 1g, scaled to represent a typical anchor pile, designed following original guidelines for floating offshore wind turbine anchors from the ABS (American Bureau of Shipping). The test programme involves selected axial load cases to investigate stable, meta-stable and unstable behaviour, and demonstrates that the factors of safety currently recommended by the ABS are insufficient, leading to premature failure of the anchor pile. However, the results show good agreement with published cyclic interaction diagrams, originally devised for the design of piles under cyclic axial loading. A set of empirical laws are derived from the experimental results to predict the number of cycles to failure and the change in pile ultimate pull-out capacity due to cyclic loading. This work suggests a revised direction for the design of anchor piles under cyclic loading.

Keywords: Floating Offshore Wind, Tension Leg Platform, Anchor Pile Design, Cyclic Loading, 1g Testing, Sand

INTRODUCTION

As the offshore wind industry expands into deeper waters, the superstructures and foundations of fixed-bottom offshore wind turbines are becoming increasingly large and expensive. Floating offshore wind turbines (FOWTs) provide a promising solution to accessing deeper waters, and their technological development is of increasing importance. However, while floating wind farms are technically feasible, the experience and knowledge in relation to their technology and design is still very much in its infancy.

Anchors and mooring systems could represent over 10% of the capital expenditure of an installed farm, and therefore optimized and robust designs could have a positive impact on the future developments of floating wind (The Carbon Trust, 2015). As floating wind develops, the design of anchors to severe long-term repeated cyclic environmental loads will be of preeminent concern, with very little work presently published in literature to assess their design and how it might affect the fatigue life of the mooring lines and floating structure. Some early work on axial pull-out capacity of piles was reported by Madabhushi and Haigh (1998). Current design guidelines mostly rely on knowledge-transfer from oil and gas floating platforms (e.g. ABS (2013)), and fixed-bottom wind turbine foundations (e.g. DNV-GL-ST-0119 (2021), DNV-GL-ST-0126 (2018)).

This paper focusses on the design of anchor piles in sand for use with Tension Leg Platforms (TLPs, Figure 1(a)). TLPs are one of the promising floating offshore wind structure types, and comprise highly buoyant platforms which are tethered to the seabed by high tension vertical tendons attached to anchors. In sandy soils, anchor piles are a good anchor type to tether the TLP (ABS, 2013). External forces on the TLP such as the wind, waves and current create a purely tensile cyclic load on the anchor (Figure 1(b)). This cyclic load could cause excessive uplift displacement if not accounted for in design.

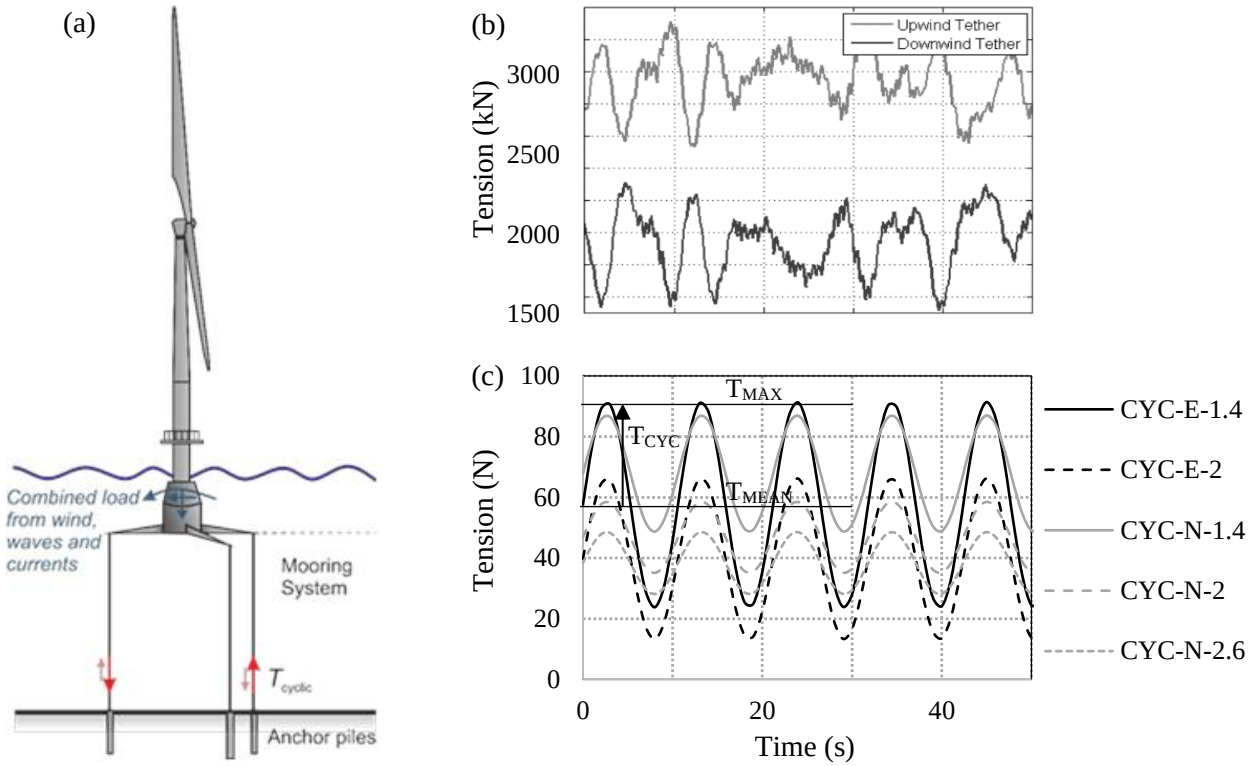

Figure 1. *(a) Schematic representation of a TLP-supported FOWT (b) Realistic tendon tension load, operating conditions (Crozier, 2011) (c) Idealised tensions applied during test programme; definitions of T_{MAX}, T_{CYC} and T_{MEAN} shown on test CYC-E-1.4*

This paper presents experimental work to further understand the behaviour of anchor piles in sand for TLPs. A range of one-way constant amplitude cyclic axial loads are applied to a model pile in sand at 1g, designed to represent a typical anchor pile for a TLP (ABS, 2013). The pile displacement is measured and the test results are used to (i) assess factor of safety methods for cyclic design, and (ii) compare with published stability diagrams for axially loaded piles (Jardine & Standing, 2012; Tsuha, et al., 2012). The results are also used to provide the basis for a set of empirical laws which can be used to estimate (i) the number of cycles sustained by the pile before failure, and (ii) the change in the pile's ultimate holding capacity.

Traditional Anchor Design Methods

The design of anchor piles under axial tensile loads is commonly achieved using the same design practices as for (mono)piles, typically using the *t-z* curves method (DNV-GL, 2018; 2021). However, there is limited recommendation with regards to how the effects of cyclic loading should be accounted for, as this is not a critical loading condition for offshore wind monopiles.

The effect of cyclic loads can be accommodated for through the estimation of the ultimate holding capacity in the mooring line used for monotonic design, multiplied by factors of safety that are based on experience and conservative assumptions (Puech, 2013). This commonly accounts for all cyclic case scenarios, and aims at estimating which would be the worst through weighting via load factors. DNV-GL (2021) recommends estimating the design anchor resistance from a sum of the characteristic mean and dynamic tensions, multiplied by load factors in the range of 1.0 to 2.86 (see DNV-GL-ST-0119 pp. 102,108-111). The design method for monotonic loading (traditionally the t-z curves method) is then used. The ABS design method for TLP anchor piles (ABS, 2013) is similar. In its method the ultimate holding capacity of the anchor pile, T_{ULT}, is determined by multiplying the maximum expected load on the pile for a given load case, T_{MAX}, by the factor of safety, FOS, for that specific load case. T_{ULT} is then taken as the maximum of all the obtained values as shown in Equation 1.

$$T_{ULT} = \max(\text{All } T_{MAX} \times \text{FOS}) \quad (1)$$

The factor of safety FOS is equal to 3 for normal loading and 2.25 for extreme loading. This definition can also be used to define the maximum tolerable cyclic load on an anchor pile, and will be used in this respect in the following

Cyclic Stability Diagrams

A better design tool for the cyclic axial loading of piles is an interaction diagram, also called a cyclic stability diagram. Cyclic stability diagrams have mainly been developed for pile design to axial cyclic loading, and recent contributions from the SOLCYP project (SOLCYP, 2012) have enabled the establishment of a framework for both sand and clay, for piles subjected to both tensile and compressive cyclic loads, based on both field and laboratory tests (Puech, 2013). These diagrams, of which the principles are summarized in Figure 2, synthesise the effect of the mean and cyclic loading amplitude T_{MEAN} and T_{CYC} (Figure 1(c)), on the number of cycles to a pile's failure, N_f. The failure criteria typically taken to define these zones are whichever occurs first of a pile head displacement, δ, exceeding 10% of the pile diameter, or a pile head displacement displaying a sudden rapid increase, indicating shaft failure (Silva, et al., 2013). Cyclic load case scenarios are then identified to be in one of three zones:

- stable (i.e. "safe") zone: characterised by a slow increase of accumulated displacements that effectively stabilize after a certain number of cycles, typically $N_f > 1000$.
- meta-stable zone: where a rapid increase in deflection and pile failure is observed for cycle number $100 < N_f < 1000$.
- unstable zone: typically characterised by rapid accumulation of displacement and abrupt reduction in ultimate holding capacity at low cycle number, i.e. $N_f < 100$.

The interaction diagram design tool can therefore be used to ensure that the amplitude of cyclic loading applied to a pile will only ever lead to safe stable behaviour (Jardine & Standing, 2012; Tsuha, et al., 2012).

Empirical Evolution laws

Jardine and Standing (2012) data also form the basis for the derivation of a simple empirical formula for predicting the reduction of a pile's shaft resistance, and therefore the reduction in its ultimate holding capacity, ΔT_{ULT}, with cycle number, N as shown in Equation 2 (Andersen, Puech, A, & Jardine, 2013).

$$\frac{\Delta T_{ULT}}{T_{ULT}} = A\left(B + \frac{T_{CYC}}{T_{ULT}}\right) N^C \qquad (2)$$

A, B and C are constants equal to -0.126, -0.1 and 0.45 respectively, and are derived to fit the data from Jardine and Standing (2012).

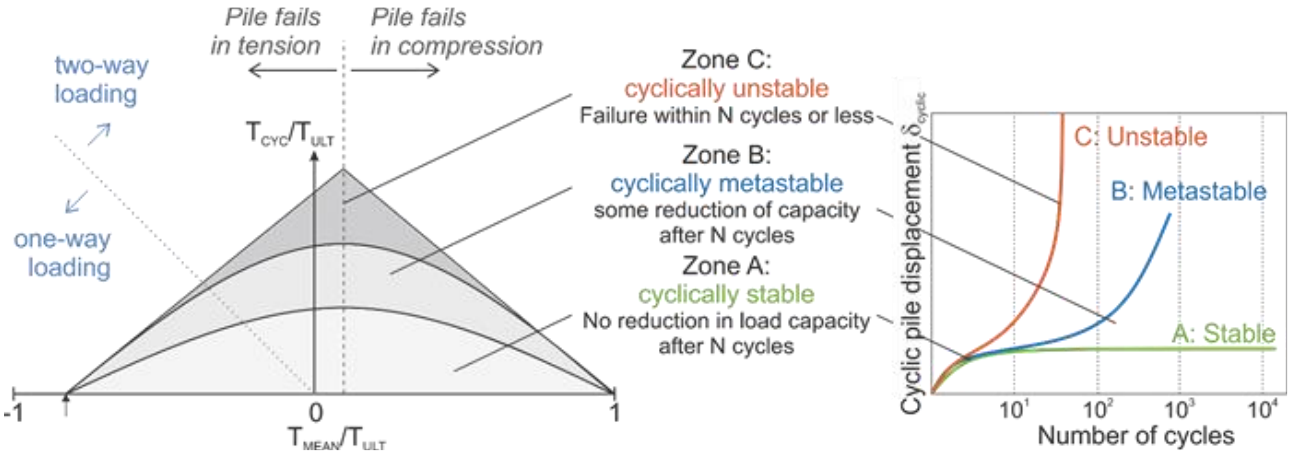

Figure 2. *Principles of cyclically loaded stability diagrams for axially loaded piles*

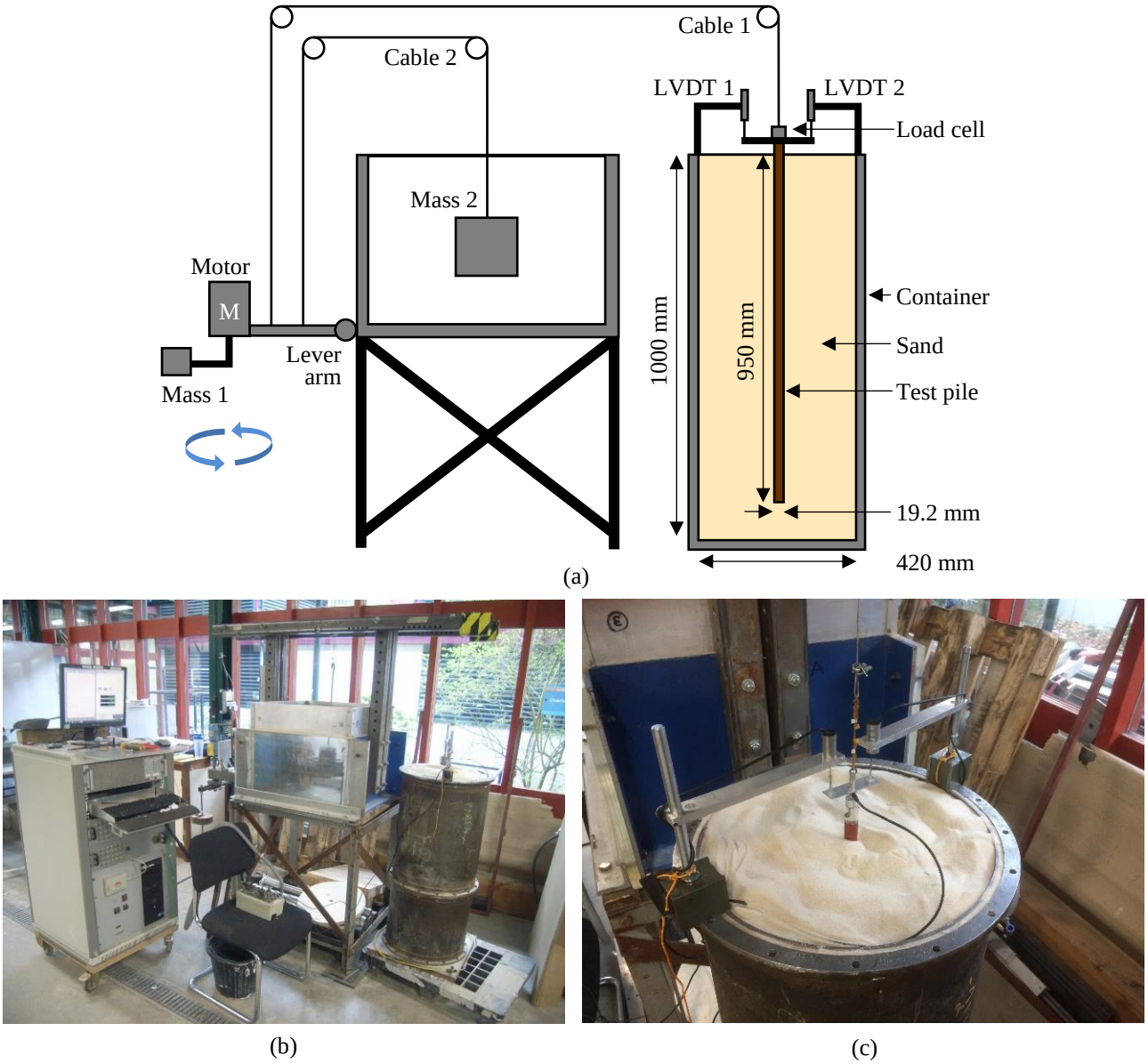

Figure 3. *(a) Schematic of Test Rig (b) Test Rig and data acquisition computer (c) LVDT, load cell and pile set-up*

EXPERIMENTAL METHOD

Testing equipment

The cyclic test rig used in this study was originally designed and developed by Rovere (2004) to apply cyclic axial loading on small-scale model suction piles in sand, and was then modified to investigate the lateral loading of piles in sand (Leblanc, Houlsby, & Byrne, 2010a; 2010b; Abadie, 2015; Abadie, Byrne, & Houlsby, 2018). It was adapted here to perform long-term cyclic axial loading on a long slender pile, with the set-up shown in Figure 3.

One-way cyclic loading was applied through a motor driving a rotating mass, Mass 1, located at the end of a lever arm. Mass 2 is chosen to balance the weight of the supporting arm and motor, in order to apply a one-way sinusoidal tensile load on top of the pile via Cable 1. The motor frequency is 0.106 Hz, mimicking the frequency of wave loading. Two LVDTs located at the pile head enable to measure the pile deflection, with data acquired via the DASYLab software. A load cell located along Cable 1 enable to check the applied load onto the pile.

Table 1. *Properties of Hostun Sand (Mitrani, 2006; Heron, 2014)*

Property	Description	Value
e_{min}	Minimum void ratio	0.555
e_{max}	Maximum void ratio	1.01
G_s	Specific gravity	2.65
ϕ_{crit} *(degrees)*	Critical angle of friction	33
d_{50} *(mm)*	Mean particle size	0.424
C_u	Uniformity coefficient	1.67

Table 2. *Anchor Pile Properties*

Property	Description	Acrylic pipe	Acrylic pipe + sand paper
L (mm)	Length	950	950
D (mm)	Total pile outer diameter	18	19.2
t (mm)	Pile wall thickness	3.0	3.6
L/D	Aspect ratio	52.8	49.5
λ	Dimensionless axial stiffness	160	178

Sample Properties

The experimental tests were conducted in dry Hostun sand HN31 (Table 1) at 1g to mimic the drained conditions typically achieved for long-term wave-induced cyclic loading. In order to limit the effects of dilation at this very low confining stresses, a repeatable low relative density D_R = 8% was achieved by pouring the sand manually from a very low drop height. The pile was "wished in place" by pouring the sand carefully around it in order to preserve the soil-shaft interface and suppress the effects of friction fatigue from installation. This also enabled more consistent and repeatable results in terms of measured ultimate holding capacity, T_{ULT}, in the sand.

Pile Geometry

The ABS design guidelines (ABS, 2013) recommend an anchor pile aspect ratio L/D = 50 in sand to tether TLP offshore wind turbines. At model-scale, the pile dimensions were limited by the size of the laboratory container (Figure 3), to a value of L = 950 mm and a pile diameter of D ≈ 19 mm in order to leave a reasonable clearance of 2.6 D between the pile and the bottom of the container.

The ABS also recommends a diameter over thickness ratio D/t = 40 for steel piles to ensure sufficient axial stiffness. However, achieving this ratio would have led to an unreasonably thin steel pipe, that are commercially unavailable (e.g. t ≈ 0.47 mm). Instead, an acrylic pipe with wall thickness t = 3.0 mm was chosen, and the dimensionless axial stiffness ratio, λ, was scaled adequately to match full-scale anchor piles (Randolph & Wroth, 1978).

$$\lambda = \frac{4\pi E t}{D G_0} \tag{3}$$

Where E is the Young's modulus and G_0 the average initial shear modulus of the sand down the pile length. λ is typically around 170 for a prototype anchor pile, designed following the ABS guidelines (Jardine & Standing, 2000). Using the framework from (Hardin & Drnevich, 1972) to assess a value of G_0 = 13.1 MPa of

Table 3. *Test programme and results overview (see definition of load characteristics in Figure 1(c))*

Test	$\frac{T_{MAX}}{T_{ULT}}$	$\frac{T_{CYC}}{T_{MAX}}$	$\frac{T_{CYC}}{T_{ULT}}$	$\frac{T_{MEAN}}{T_{ULT}}$	FOS T_{ULT}/T_{MAX}	Number of cycles	N_i	$N_{0.1D}$	N_a	N_s	N_f	Response
PO-1	Monotonic Pull-out				-	1	-	-	-	-	-	-
PO-2	Monotonic Pull-out				-	1	-	-	-	-	-	-
PO-3	Monotonic Pull-out				-	1	-	-	-	-	-	-
CYC-E-1.4	0.7	0.4	0.3	0.5	1.4	55	20	31	38	55	31	Unstable
CYC-N-1.4	0.7	0.2	0.2	0.5	1.4	1869	330	717	1103	1869	717	Meta-stable
CYC-E-2	0.5	0.4	0.2	0.3	1.9	356	130	168	280	356	168	Meta-stable
CYC-N-2	0.5	0.2	0.1	0.4	2.1	8037	>8037	7073	n/a	>8037	7073	Stable
CYC-N-2.6	0.4	0.2	0.1	0.3	2.6	8556	>8556	>8556	n/a	>8556	>8556	Stable

the laboratory sample, an acrylic pipe of dimensions provided in Table 2 was selected, providing a value of $\lambda = 160$.

Finally, the shaft-soil interaction obtained with this choice of pipe material was too smooth to mimic the tensile behaviour typically obtained at higher confining stresses. To improve coupling at the interface, the acrylic pipe was coated using P60 sandpaper (0.6 mm thick), increasing the pile outer diameter to 19.2 mm and leading to the final anchor pile dimensions listed in Table 2.

Test Programme

The test programme involved a series of monotonic pull-out tests, aimed at determining both the ultimate holding capacity T_{ULT} of the test pile in the sand, and the repeatability of the testing procedures (PO-1,2,3, Table 3). This was followed by a series of cyclic loading tests, for which the idealized input signal is provided in Figure 1(c) and Table 3.

The range of one-way cyclic load cases was chosen to investigate the effects of both the load amplitude (T_{CYC}) and the load magnitude (T_{MAX}), by varying the dimensionless loading ratios T_{CYC}/T_{MAX} and T_{ULT}/T_{MAX} (which corresponds to the load factor of safety FOS of Equation 1). The two load amplitudes tested, correspond to a "normal" and "extreme" case (Suzuki, et al., 2011; ABS, 2012; Crozier, 2011; Matha, 2009), and have amplitudes T_{CYC}/T_{MAX} of 0.2 and 0.4 respectively. Three factors of safety were tested: FOS = 2.6, 2.0 and 1.4. The two larger ratios are as close as experimentally possible to the values recommended in the ABS design method for extreme and normal loading (3.0 and 2.25 respectively), both expected to lead to a stable behaviour according to the ABS. The ratio of 1.4 was added to this study to ensure an unstable cyclic behaviour for later comparison with the work on stability diagrams by Tsuha *et al.* (2012).

The stable cyclic tests were stopped after ~8000 cycles, which was enough cycles to ensure a stable behaviour (Jardine & Standing, 2012). They were then followed by a monotonic pull-out test to estimate the degradation of the ultimate holding capacity caused by cyclic loading and friction-fatigue.

MONOTONIC RESPONSE

The results of the monotonic tests are shown in Figure 4. The differences observed between the tests evidence some experimental error caused by model preparation. However, the discrepancy is within the expected experimental error for this type of 1g test. The curves display a peak response, which naturally defines the ultimate holding capacity of the pile $T_{ULT} = 125.2 \pm 13.9$ N. This is followed by a rapid softening of the pile response, caused by a loss of shaft resistance that induces a loss in tension in Cable 1 once the pile has reached capacity.

The API pile design method (API, 2000) was used to make predictions of the ultimate holding capacity of the test pile, considering two cases: (i) a smooth pile surface ($T_{ULT,API,S}$), with a soil-pile friction angle of $\delta = 15^{\circ}$ and (ii) a more realistic prediction of the sand-coated pile used in this paper, considering a rough pile surface, ($T_{ULT,API,R}$), with $\delta = 22^{\circ}$ (Tomlinson, 2001). This gives ultimate capacities of $T_{ULT,API,S} = 80.3$ N and $T_{ULT,API,R} = 119.3$ N (reported in Figure 4).

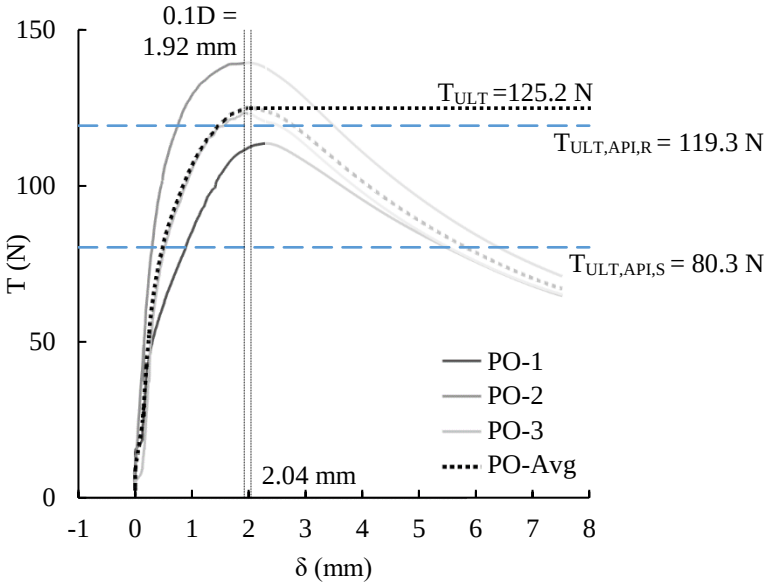

Figure 4. *T-δ response of the monotonic pull-out tests PO-1,2,3*

CYCLIC RESPONSE

Figure 5 shows the comparative tension-displacement curve response of an unstable, meta-stable and stable case. The number of cycles that can be sustained by the pile during cyclic loading can be defined as follows, depending on what is most critical for design (Figure 6, Table 3):

- N_i is the number of cycles before a change from stable to meta/un-stable behaviour, defined by the **i**nflexion point, after which the second derivative of the δ-N curve becomes positive.
- $N_{0.1D}$ is the number of cycles after which the pile displacement is greater than 0.1D, i.e. 1.92 mm.
- N_a is the 'point of **a**cceleration' after which the pile begins to show a noticeable increase in displacement rate, signalling impending shaft failure. It is defined as the point at which the $\log(\Delta\delta/\delta_s)$–$\log(N)$ curve of each cyclic test crosses above its trendline Figure 6(b).
- N_s is the point of shaft failure after which the pile can no longer sustain T_{MAX}.
- N_f is the point of cyclic failure, adapted from the definition chosen by Tsuha *et al.* (2012) in cyclic stability diagrams. Here, cyclic failure is defined as the number of cycles required to either (i) reach a pile displacement of 10% of the pile diameter ($N_f = N_{0.1D}$ in this case), or (ii) corresponding to pile axial failure, caused by a very sharp increase in pile displacement ($N_f = N_a$) and subsequent pile shaft failure ($N_f = N_s$):

$$N_f = \min\left(N_{0.1D}, N_a, N_s\right) \tag{4}$$

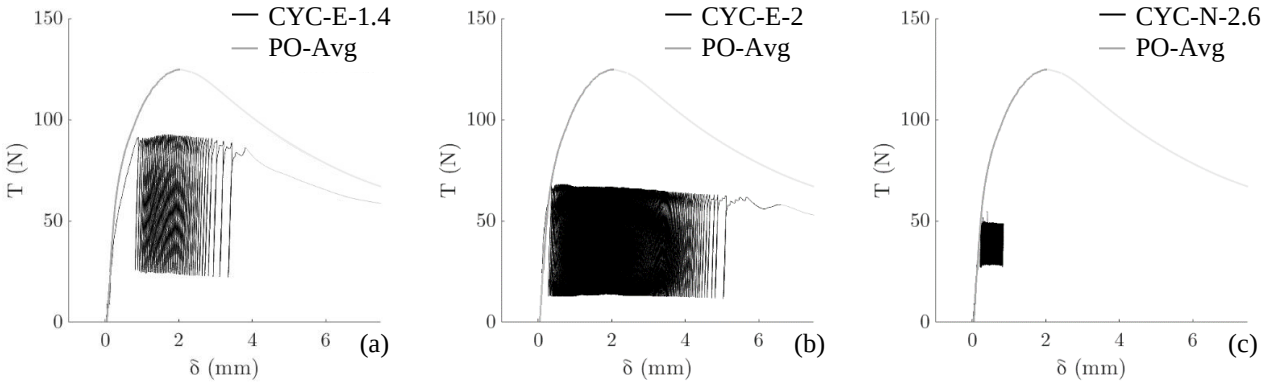

Figure 5. *T-δ response of: (a) test CYC-E-1.4, unstable (b) test CYC-E-2, meta-stable (c) CYC-N-2.6, stable (stopped after 8556 cycles)*

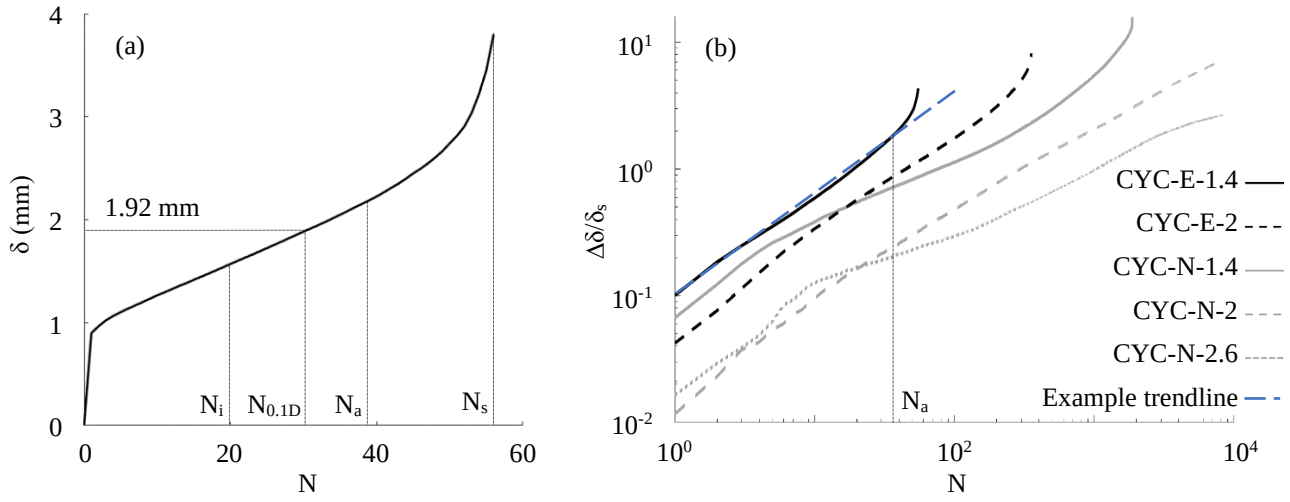

Figure 6. *Evolution of pile head displacement with cycle number (a) Test CYC-E-1.5, and definition of N_i, $N_{0.1D}$, and N_s, (b) Compared accumulated pile displacement $\Delta\delta$ of all 5 cyclic tests, with an example trendline plotted for test CYC-E-1.4 used to define N_a*

This definition enables comparison with data in the published domain, but offers a more conservative estimate than the definition adopted by Tsuha *et al.* (2012). These definitions are illustrated in Figure 6(a), together with the evolution of the pile head displacement with cycle number. In Figure 6(b) $\Delta\delta$ is defined as the cyclic pile head displacement relative to the initial monotonic displacement. It is normalised by δ_s which is the pile head displacement resulting from the application of T_{MAX} in a static load test (PO-Avg).

Factors of Safety

First, the results can be used to assess factors of safety methods for TLP pile anchors in sand. Table 3 provides an overview of the results obtained for the tests. The selected factors of safety chosen for extreme (CYC-E) and normal (CYC-N) load events must ensure a stable behaviour at all times. The results show that a factor of 2.6 for "Normal" – i.e. long-term operational – loading is sufficient (see test CYC-N-2.6 in Table 3). However, a factor of safety of 2 for extreme load (CYC-E-2) is likely to be unconservative if a stable behaviour is targeted. In practice, it would be best to assess the number of cycles expected for each load type, and ensure that N_f is reasonably smaller than this critical number for this load case. This is what cyclic stability diagrams provide.

Cyclic Stability Diagrams

Figure 7 shows the experimental results from Jardine and Standing (2012) also reported by Tsuha *et al.* (2012) for one-way tensile cyclic loading tests. The large-scale piles were tested with the facilities of the GOPAL (Grouted Offshore Piles Alternating Loading) research project, on 7 open-ended driven piles in dense Dunkirk sand ($D_R \approx 75\%$), of L = 19 m in length and D = 457 mm in diameter (L/D = 41.6), and plugged at ~60% of the embedded length.

The results obtained in this paper have been added to the diagram for comparison. The numbers labelled on the figure correspond to the number of cycles at failure, N_f.

The two sets of results show good agreement, and the interaction diagram correctly predicts the stable, meta-stable or unstable behaviour of all but one cyclic test, CYC-E-1.4, which is however aligned with another meta-stable test that failed around the same number of cycles in this zone. The exact stable, meta-stable and unstable zones and cycle numbers are likely to vary with soil conditions and pile parameters (Tsuha, et al., 2012), and further work is needed to improve this data base for future design.

Prediction of number of cycles to failure

In addition to stability diagrams, predicting the number of cycles to failure can be aided by empirical equations. The results in Table 3 clearly show that an increase in the amplitude of cyclic loading T_{CYC}/T_{MAX}, or a decrease

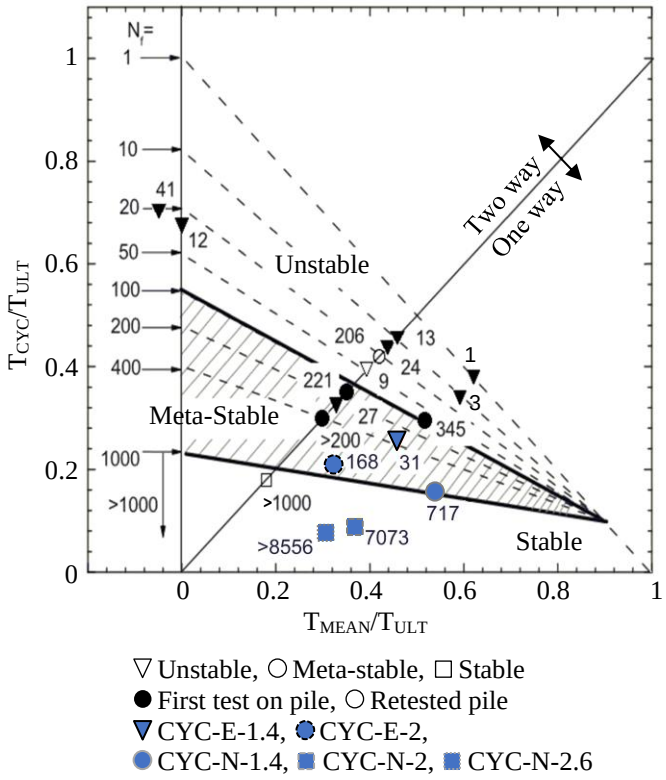

▽ Unstable, ○ Meta-stable, □ Stable
● First test on pile, ○ Retested pile
▼ CYC-E-1.4, ● CYC-E-2,
● CYC-N-1.4, ■ CYC-N-2, ■ CYC-N-2.6

Figure 7. *Cyclic stability diagram with the number of cycles to failure N_f marked from Richard and Standing (2012) and reported by Tsuha et al. (2012) and superimposed with this test campaign's results.*

in the factor of safety T_{ULT}/T_{MAX}, both have a detrimental effect on the value of N_f. Jardine and Standing (2012) demonstrated that the ratio T_{CYC}/T_{ULT} is the most important load ratio driving the response of the pile (e.g. Equation 2). A power law was fitted to the experimental results for $N_f = N_{0.1D}$ as a function of T_{CYC}/T_{ULT}, with the results shown in Figure 8:

$$N_f = 0.06 \left(\frac{T_{CYC}}{T_{ULT}}\right)^{-5} \tag{5}$$

The data from Jardine and Standing (2012) and Tsuha *et al.* (2012) are also displayed in Figure 8 for comparison. The difference in the results can in part be explained by the more conservative approach adopted in these two studies than the definition chosen for Equation 4 in this paper. Equation 5 can be used to directly provide the threshold values for which T_{CYC}/T_{ULT} enables stable (0.14) and meta-stable (0.23) behaviours. Safe stable behaviour therefore corresponds to a factor of safety of 1.24 for the normal load case (for which $T_{CYC}/T_{MAX} = 0.2$), and 2.48 for the extreme load case (for which $T_{CYC}/T_{MAX} = 0.4$).

Change in pull-out capacity

Figure 9 shows the results of the pull-out tests following the stable cyclic loading tests CYC-N-2.6 and CYC-N-2. In both tests T_{ULT} degraded from 125.2 to 99.3 N ($T_{ULT,DEG}$), a 21% reduction in strength (ΔT_{ULT} = 25.9 N). This is typical of piles subjected to cyclic (wave) loading, where the shaft capacity typically reduces massively due to friction fatigue during cyclic loading (Poulos, 1989; Dejong, Randolph, & White, 2003).

For the unstable and meta-stable tests, the test pile experienced shaft failure during cycling when T_{ULT} degraded to such an extent that $T_{ULT} = T_{MAX}$, and $\Delta T_{ULT} = T_{MAX} - T_{ULT}$. The results were compared with Equation 2, and the values of A, B and C optimised using linear regression (Figure 9, Equation 6).

$$\frac{\Delta T_{ULT}}{T_{ULT}} = -0.26 \left(-0.08 + \frac{T_{CYC}}{T_{ULT}}\right) N^{0.43} \tag{6}$$

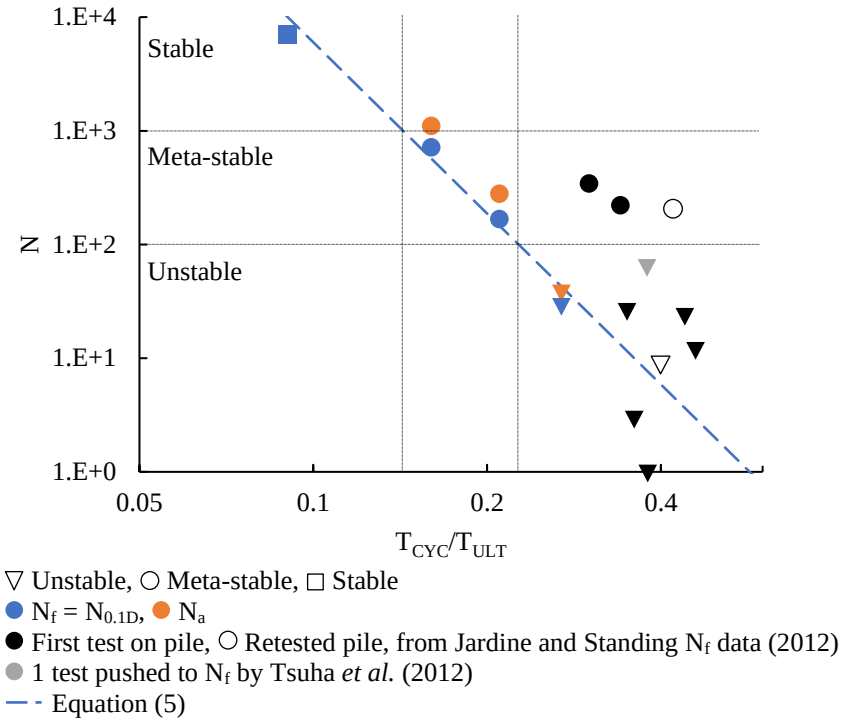

Figure 8. *Evolution of cycle number as a function of T_{CYC}/T_{ULT} for this campaign's test results and the one-way cyclic results from Jardine and Standing (2012) and Tsuha et al. (2012). The trendline of Equation (5) is also plotted.*

The constants A, B and C are of the same order of magnitude as that obtained from Jardine and Standing (2012) (-0.126, -0.1 and 0.45 respectively).

Equation 6 shows that for very long-term cyclic loads characterised by $T_{CYC}/T_{ULT} < 0.08$, no cyclic degradation of the ultimate holding capacity is expected. This would correspond to typical operational conditions of the FOWT in quiet sea.

CONCLUSIONS

This paper presents the results of an experimental campaign aimed at investigating the suitability of existing design methods for anchor piles subjected to tensile cyclic loads. The results show that the use of large factors of safety, as recommended in current design guidelines might be sufficient for certain load case scenarios but neither provides an accurate design method, nor accounts for cycle number.

A more rigorous approach consists of using stability diagrams, from which empirical evolution laws can be derived for design. The framework introduced by Jardine and Standing (2012) and Tsuha *et al.* (2012) can be directly applied for more accurate design and provides a reasonable assessment of (i) the number of cycles to failure, and (ii) the degradation of the ultimate holding capacity of the anchors. Further work using centrifuge modelling would enable the completion of these models at representative soil stress levels and pile dimensions.

ACKNOWLEDGEMENT

The authors are thankful for the support of the Schofield Centre in conducting this project, and the support provided while conducting the last tests at the start of the COVID-19 pandemic. The authors are also thankful for the fruitful discussions with Tobias Möller.

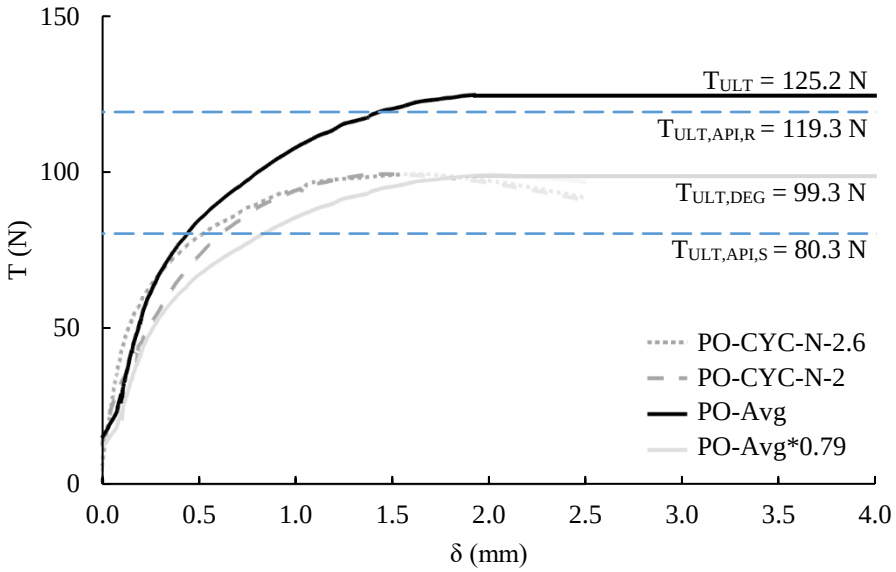

Figure 9. *Pull-out tests after stable cyclic loading, with PO-Avg scaled to match the curves*

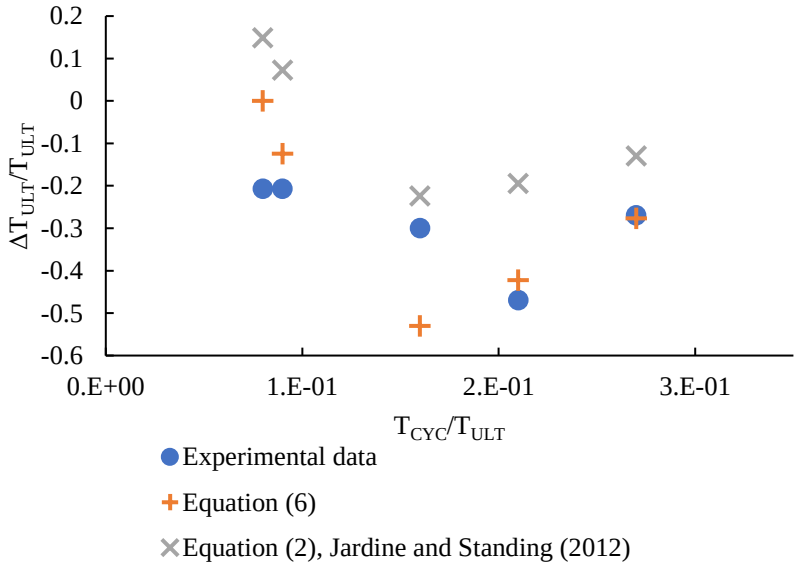

Figure 10. *Prediction of the change in ultimate capacity following the framework from Jardine and Standing (2012)*

REFERENCES

Abadie, C. (2015). *Cyclic Lateral Loading of Monopile Foundations in Cohesionless Soils.* Oxford: University of Oxford.

Abadie, C., Byrne, B. W., & Houlsby, G. T. (2018). Rigid pile response to cyclic lateral loading: laboratory tests. *Géotechnique*, 1-41.

ABS. (2012). *Floating Wind Turbines.* Houston: American Bureau of Shipping (ABS).

ABS. (2013). *Offshore Anchor Data for Preliminary Design of Anchors of Floating Offshore Wind Turbines.* Houston: American Bureau of Shipping (ABS).

Andersen, A. K., Puech, A, A., & Jardine, R. J. (2013). Cyclic resistant geotechnical design and parameter selection for offshore engineering and other applications . Paris: ISSMGE Technical Committee TC 209.

API. (2000). *API-RP-2A: Recommended Practice for Planning, Designing and Constructing Fixed Offshore Platforms.* Washington: API.

Crozier, A. (2011). *Design and Dynamic Modeling of the Support Structure for a 10 MW Offshore Wind Turbine.* Trondheim: Norwegian University of Science and Technology.

Dejong, J. T., Randolph, M. F., & White, D. J. (2003). Interface Load Transfer Degradation During Cyclic Loading: A Microscale Investigation. *Journal of the Japanese Geotechnical Society*, 81-93.

DNV-GL. (2018). *DNVGL-ST-0126: Support structures for wind turbines.* Oslo: DNV-GL.

DNV-GL. (2021). *DNV-GL-ST-0119: Floating Wind Turbine Structures.* Oslo: DNV-GL.

Hardin, B., & Drnevich, V. (1972). Shear Modulus and Damping in Soils: Design Equations and Curves. *Geotechnical Special Publication*, 667-692.

Heron, C. (2014). The Dynamic Soil Structure Interaction of Shallow Foundations on Dry Sand Beds. University of Cambridge, Geotechnical Group.

Jardine, R. J., & Standing, J. R. (2000). *Pile load testing performed for HSE cyclic loading study at Dunkirk, France - Volume 1.* London: Health and Safety Executive.

Jardine, R. J., & Standing, R. J. (2012). Field axial cyclic loading experiments on piles driven in sand. *Soils and Foundations, 52*(4), 723-736.

Leblanc, C., Houlsby, G. T., & Byrne, B. W. (2010a). Response of stiff piles in sand to long-term cyclic lateral loading. *Geotechnique, 60*(2), 79-90.

Leblanc, C., Houlsby, G. T., & Byrne, B. W. (2010b). Response of stiff piles to random two-way lateral loading. *Géotechnique*, 715-721.

Madabhushi, S., & S.K., H. (1998). Finite Element Analysis of Pile Foundations Subject to Pull-Out. In: Cividini A. (eds) Application of Numerical Methods to Geotechnical Problems. International Centre for Mechanical Sciences (Courses and Lectures), vol 397. (pp. 131-140). Vienna: Springer. doi:https://doi.org/10.1007/978-3-7091-2512-0_12

Matha, D. (2009). *Model Development and Loads Analysis of an Offshore Wind Turbine on a Tension Leg Platform, with a Comparison to Other Floating Turbine Concepts.* Boulder: National Renewable Energy Laboratory & University of Colorado.

Mitrani, H. (2006). Liquefaction Remediation Techniques for Existing Buildings, PhD Thesis. Univeristy of Cambridge, Geotechnical Engineering Group.

Poulos, H. G. (1989). Pile behaviour—theory and application. *Géotechnique*, 365-415.

Puech, A. (2013). Advances in axial cyclic pile design: contribution of the SOLCYP project . Paris: ISSMGE Technical Committee TC 209 .

Randolph, M., & Wroth, C. (1978). Analysis of deformation of. *Journal of the Geotechnical Engineering Division*, 1465-1488.

Rovere, M. (2004). Cyclic loading test machine for caisson suction foundations. Oxford.

Silva, M., Foray, P., Rimoy, S., Jardine, R., Tsuha, C., & Yang, Z. (2013). Influence of cyclic axial loads on the behaviour of piles driven in sand . Paris: ISSMGE Technical Committee TC 209.

SOLCYP. (2012). *A Four-Year Joint Industry Project On the Behaviour of Piles Under Cyclic Loading.* London: Society of Underwater Technology.

Suzuki, K., Yamaguchi, H., Akase, M., Imakita, A., Ishihara, T., Fukumoto, Y., & Oyama, T. (2011). Initial Design of Tension Leg Platform for Offshore Wind Farm. *Journal of Fluid Science and Technology, 6*(3), 372-381.

The Carbon Trust. (2015). *Floating Offshore Wind: Market and Technology Review.* London: The Carbon Trust.

Tomlinson, M. J. (2001). *Foundation Design and Construction.* Hoboken: Prentice Hall.

Tsuha, C., Forayb, P., Jardine, R., Yang, Z., Silva, M., & Rimoy, S. (2012). Behaviour of displacement piles in sand under cyclic axial loading. *Soils and Foundations, 52*(3), 393-410.